A radiometric contouring approach to map the shoreline

Antonino Maltese*[a], Francesco Caldareri[b], Nicolò Parrino[b], Simona Todaro[b], Gino Dardanelli[a], Attilio Sulli[b]

[a]Dipartimento di Ingegneria, Università degli Studi di Palermo, Palermo, Italy

[b]Dipartimento di Scienze della Terra e del Mare, Università degli Studi di Palermo, Palermo, Italy

Keywords: Shoreline, iso-radiometry, contouring, optical, thermal, Synthetic Aperture Radar, positioning accuracy

ABSTRACT

Estimating the accurate position of the shoreline over time can be challenging. We propose a new approach to delimit the shoreline from remotely sensed images simply and accurately. This approach treats pixels as simultaneous radiometric measurements, and by examining the distance between iso-radiometry lines, it assumes the shoreline in the position where the radiometric behaviour changes more suddenly.

The analyses carried out applying this coastline extraction approach underscore its significant flexibility. Specifically, the approach yielded promising outcomes even if applied to a variety of different and dissimilar types of remotely sensed products. Indeed, the intrinsic straightforwardness and low computational load of the approach qualify it as a promising tool for time-series production.

1. INTRODUCTION

The shoreline serves as the boundary line separating terrestrial sediments from adjacent water bodies, such as seas, lakes, or rivers. Among the range of geological processes influencing the shoreline position, such as rockfall phenomena in coastal and pericoastal cliffs [1–3], the vertical variations in sea level are the one that stands as a primary driver. These vertical fluctuations are particularly impactful, serving as the dominant forcing mechanisms that shape the evolution of coastal landscapes across various spatial and temporal scales [4,5].

Examining the shoreline position represents a challenging task owing to the dynamic nature of these coastal environments. When shifts in the position of the sea coastline are considered over geological time scales, they can contribute to the formation of extensive polycyclic coastal plains or the emergence of staircased marine terraces, as observed in W-Sicily [6–8].

In contrast, at daily timescales, the lower elevation limit of the shoreline on sandy beaches influences the formation of a Low Tide Terrace (LTT), while its upper elevation limit contributes to the creation of the ordinary berm [9].

The precise location of the coastline holds substantial implications for the management and monitoring of critical anthropogenic assets. Leveraging remotely sensed products, a variety of coastline extraction approaches have been developed and those approaches can be distinguished into a few broad categories. Some standard approaches for shoreline mapping include manual or automatic digitization on orthophotos, full-field surveys using GNSS techniques, and pixel-based approaches using raster image processing.

Pixel-based approaches can be further categorized into image thresholding, water indices [10], raster-based approaches [11], and vector-based [12]. We introduce a novel methodology based on raster contouring, wherein the shoreline is delineated by treating pixels as concurrent points of radiometric remote measurements.

2. MATERIALS

A Virtual Reference Station Network Real Time Kinematic (VRS NRTK) positioning solution was employed since this solution showed a variability for North, East and Up components lower than 19 cm and a standard deviation lower than 5.4 cm compared to Static solution [13]. The approach was tested on images distributed at different spatial resolutions, between 3 and 30 m. For the optical images, the Planetscope (PS), Sentinel-2 (S2) and Landsat (LS) images were examined. The PS images were preliminarily tested in the near-infrared and red-edge bands at a spatial resolution of 3 m; the S2 images were tested in three red-edge bands, two near-infrared bands, and two short-wave infrared bands at a resolution of 20 m, while LS images were processed in the near-infrared band and two short-wave infrared bands at a resolution of 30 m. These optical images were acquired simultaneously with the GNSS positioning.

Thermal images acquired by the LS platform in day and night orbits were tested in the thermal infrared (TIR). The daytime thermal imagery sensor is carried on the LS platform to acquire daytime optical images in descending orbit. The night-time thermal images were acquired at 21:36 UTC in descending orbit, approximately 12 hours after the daytime passage. The Synthetic Aperture Radar (SAR) images were acquired from the Sentinel-1 (S1) platform in C-band with cross (VH) and co (VV) polarizations at a spatial resolution of 10 m. No S1 images were available exactly on the day of the GNSS acquisition.

3. METHODS

3.1 The proposed shoreline extraction approach

The idea behind raster-based approaches is to split the image into two clusters of pixels with different radiometric values, characterizing the sea and land, respectively (Fig. 1a). The image is raster, so the boundary between the groups is a line that follows the shape of the pixels (Fig. 1b).

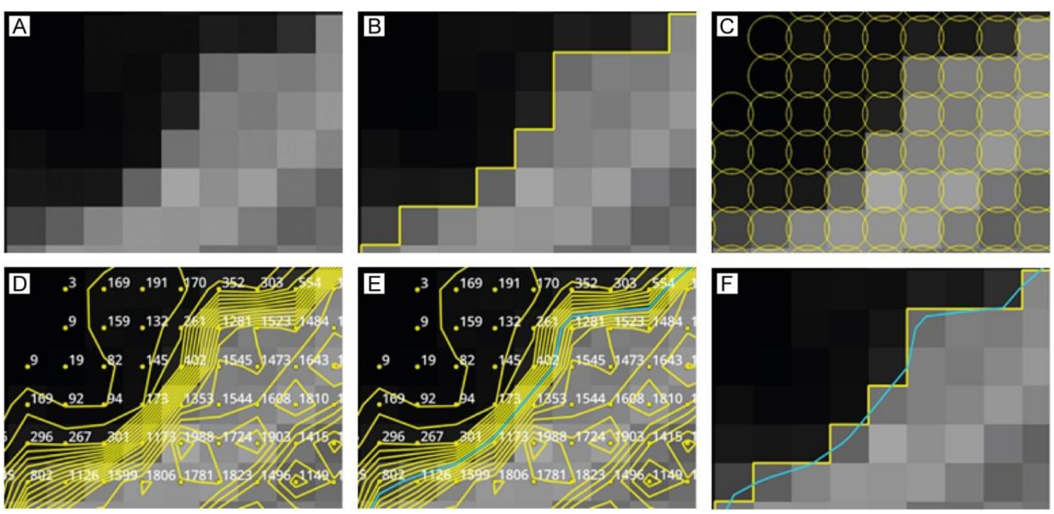

Fig. 1 - Pixel bounded versus raster contouring approaches: (a) grayscale representation of a raster band; (b) shoreline extracted with image thresholding, in yellow; (c) representation of the data through the footprint of the instantaneous field of view, yellow circles; (d) pixels digital numbers and their iso-radiometry contours, yellow values and

lines; (e) shoreline (cyan line) over imposed to the contours; pixel bounded versus raster contouring shoreline (yellow and cyan lines, respectively).

The signal can be thought of as originating from circular areas (Fig. 1c) when it is vertical and more elliptical when it is not. The proposed approach interprets the circular or elliptical surfaces originating the radiometric signal as a distribution of measurement points on a square grid (Fig. 1d).

Considering the remote sensed data as a set of points that are detected at the same time on a square grid, and if the phenomenon we interpret is related in space, we can interpolate the measurement points to mimic their spatial distribution, allowing obtaining curves of iso-radiometric values (Fig. 1d). The radiometric quantity depends on the type of imaging sensor: for instance, it can be spectral radiance or reflectance for images acquired in the sun range, it can be the surface temperature for images acquired in the thermal infrared, or it can be backscattering for images in the microwave using SAR sensors. All these radiometric quantities, indeed, change suddenly when we go from the sea to the land domains. So, in the transition between the two domains, the curves of equal radiometric values will be close to each other. We define the shoreline as the curve with the smallest distance from the previous and next curves (Fig. 1e). The coastline we get by interpolation will have a smoother variation than the one from pixel-bound approaches (Fig. 1f).

3.2 Radiometric processing methods

The optical images are calibrated in spectral reflectance and corrected by the atmospheric effect. Daytime thermal images are distributed with level two processing. In contrast, nighttime images are distributed as level-one products and, therefore, need to be calibrated in radiometric temperature by the user, the processing of S1 images is almost standard and includes applying thermal noise removal, orbit files, and terrain correction operators. Speckle degrades image quality and makes the results of any quantitative processing less accurate.

Since the speckle effect appeared evident at the pixel scale, we chose to evaluate the approach on images untreated for removal of the effect and on the same images where a speckle removal algorithm was applied. To perform a preliminary analysis of the applicability of the proposed approach on SAR images, it was chosen to filter the speckle effect by the Lee Sigma algorithm [14].

4. RESULTS

Figures 2, 3 and 4 show the results obtained by processing optical, thermal and SAR images. The berm (yellow line) and LTT (blue) were positioned via GNSS to delineate the range where the shoreline is expected to fall (red line). Results are obtained by processing red edge and NIR PS bands and S2 and LS NIR bands as shown in Fig. 2.

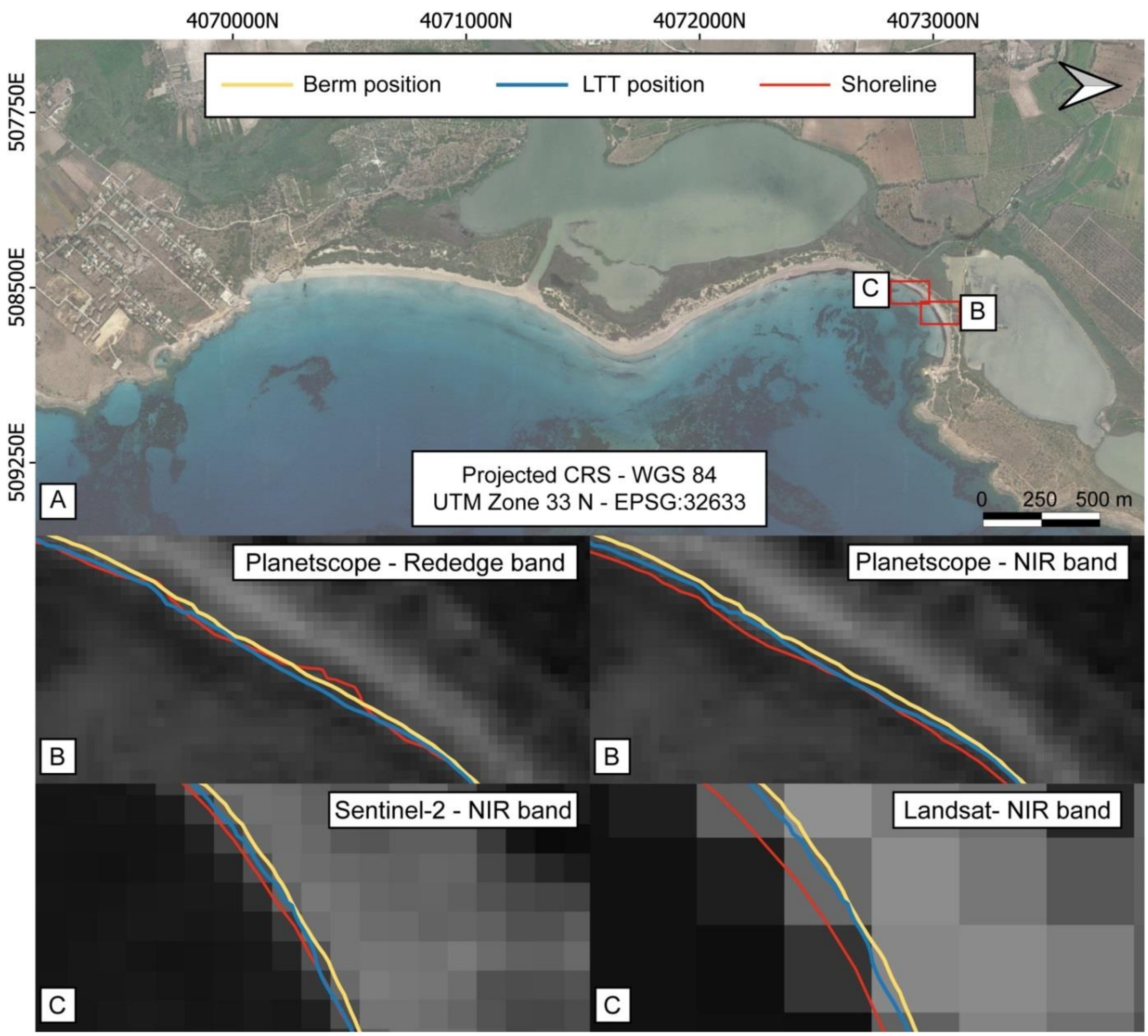

Fig. 2 - True colour composition of the study area (panel a) and subsets (panels b and c) with grayscale representation of a PS red edge and NIR bands (panel b, left and right, respectively), S2 NIR band (c panel) and Landsat

NIR band (c panel) with over imposed the raster contouring shoreline position (red line) and the berm and the LTT positions measured via GNSS (yellow and blue lines, respectively).

The water pixels are characterized by a lower reflectance than the sand pixels in both the red edge and NIR bands. Also, results indicate seemingly similar performances in the NIR and red edge, with the shoreline often positioned closer to the LTT, with the accuracy varying with the spatial resolution.

Results obtained by processing daytime and nighttime LS TIR images are shown in Fig. 3 (lower panels). Surface temperatures are characterized by values on the submerged domain lower than those of the emerged domain;

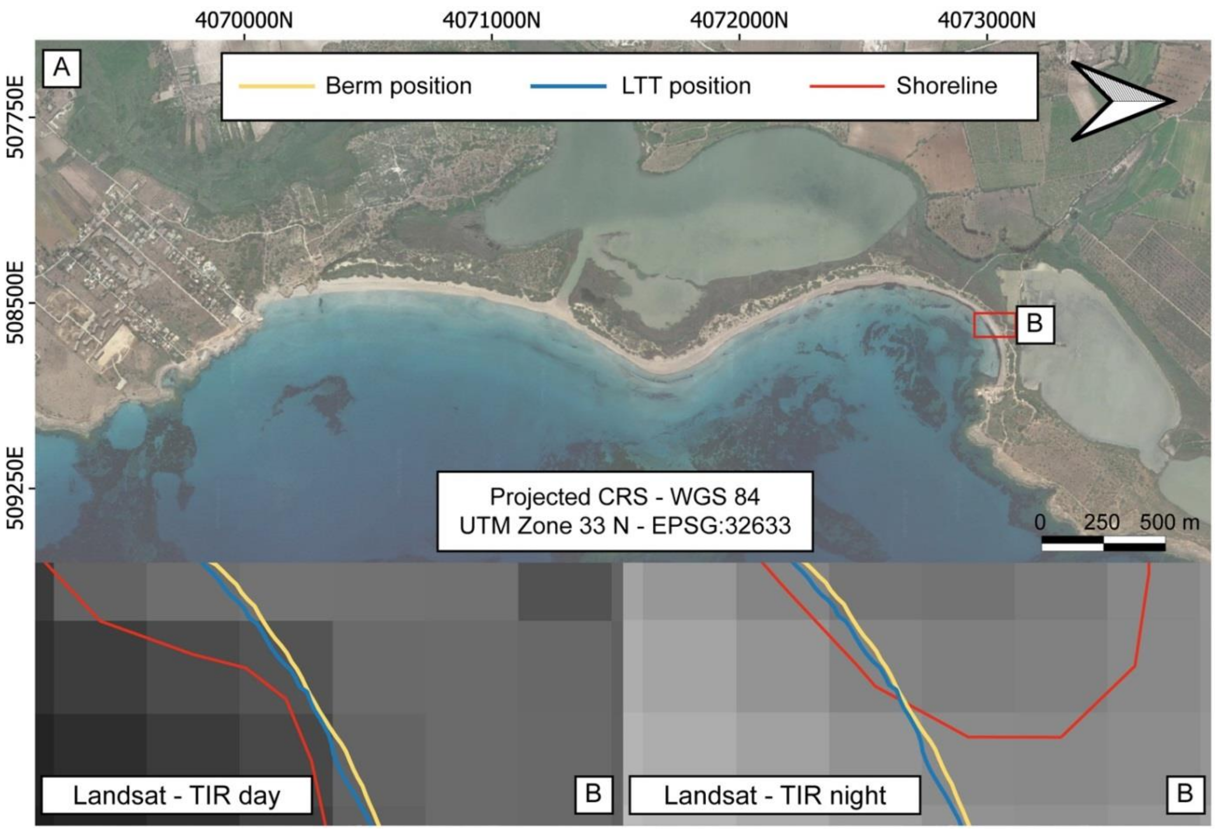

Fig. 3 - True colour composition of the study area (panel a) and subset (panels b) with grayscale representation of LS TIR daily and night bands (left and right panels, respectively), with imposed the shoreline position (red line) and the berm and the LTT positions (yellow and blue lines, respectively).

conversely, in the night-time, the pattern reverses due to the different inertia of the system [15,16], showing temperatures of the emerged domain lower than those of the submerged domain. The results indicate inaccurate positioning of the shoreline moving away from the berm and LTT.

Results obtained by processing S1 SAR images in VV and VH polarizations are shown in Fig. 4.

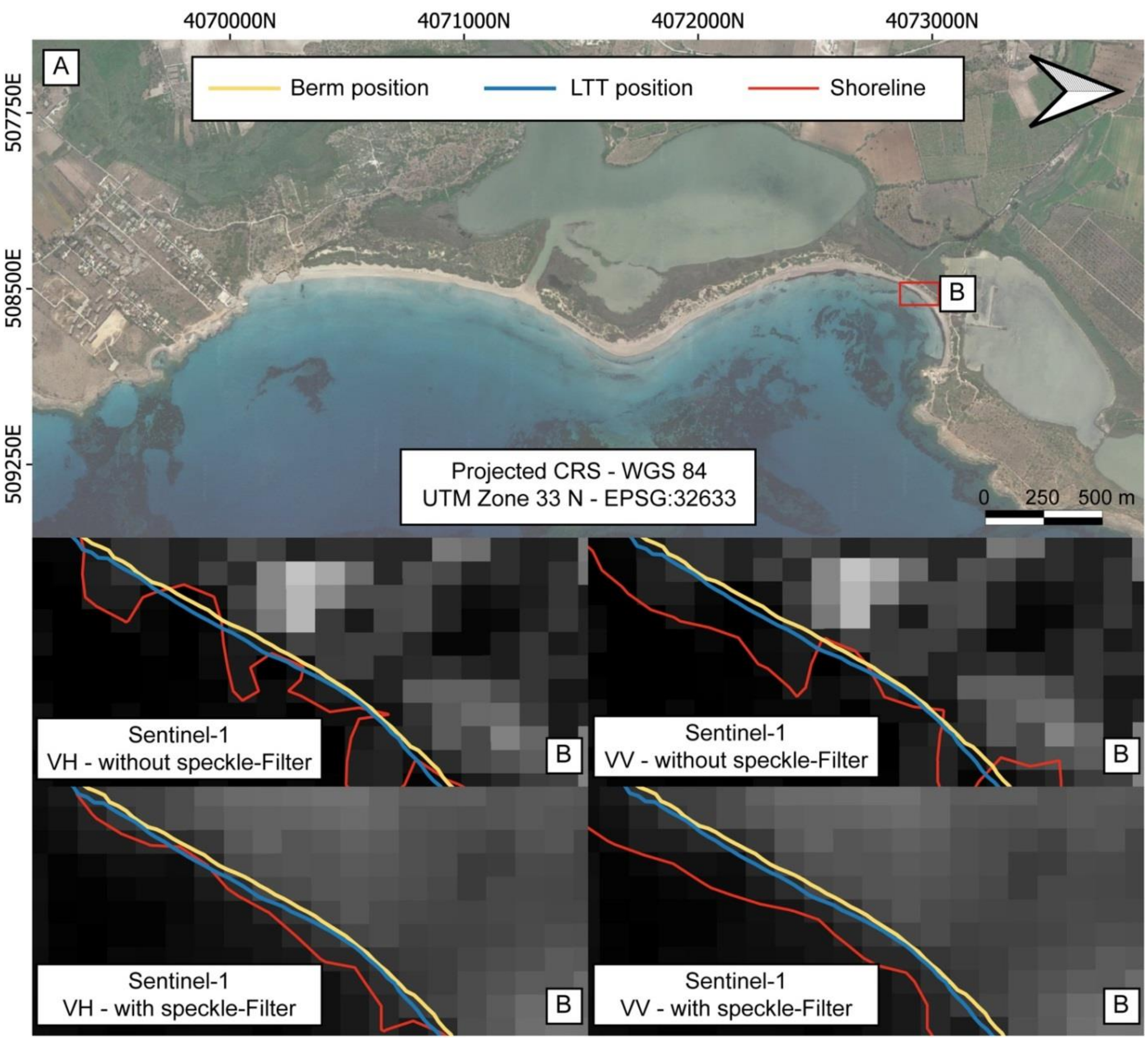

Fig. 4 - True colour composition of the study area (panel a) and subset (panels b) with a grayscale representation of the 2022-07-22 S1 cross and co-polarisation bands without speckle removal (b top left and right panels, respectively) and

with speckle removal (b lower left and right panels, respectively), with over imposed the shoreline position (red line) and the berm and the LTT positions (yellow and blue lines, respectively).

The pixels backscattering on the marine domain appears lower and more uniform than on the pixels of the beach and generally of the terrestrial domain. Following the application of the de-speckle filter, pixels of the terrestrial domain also appear uniform. Also, the shoreline extracted on the images uncorrected by the speckle effect appears highly articulated and fragmented, as well as distant from the berm – LTT lines.

The approach applied to optical images achieves variable accuracies, with metrics improving as the spatial resolution improves. The algorithm's performances on the NIR and red edge bands are similar and better than those using the SWIR bands. The least accurate results are obtained by processing thermal images, with an average distance of ~ 22 − 35 m, and worse performance is obtained using night-time thermal images. The average performance of the approach on SAR images corrected by the speckle effect (μ = ~24 m, σ = ~ 1 m) and better than achieved by not filtering out the speckle effect (μ = ~7 m, σ = ~ 0.3 m).

5. DISCUSSION AND CONCLUSIONS

The influence of spectral bands and spatial resolution on the accuracy of the methodology should be quantified. Additionally, the behaviours of the spectral signature of sand under varying water content conditions and the impact of the water column's diffuse attenuation on shoreline positioning require exploration. Another pertinent query is how the georeferencing or orthorectification accuracy of satellite products influences the precision of shoreline positioning across different spatial resolutions. Furthermore, the effects of sand grain size and consequent beach slope on achievable accuracy at various spatial resolutions merit examination. It is also necessary to highlight any critical aspects of the approach under suboptimal sea and weather conditions and any critical aspects related to coastal morphology.

Although we have decided to continue testing the methodology with optical image data, this does not mean the research on the use of thermal images and SAR should be abandoned. It is expected that high-resolution commercial imagery in thermal infrared and SAR will soon be available. The availability of high-resolution thermal infrared and microwave images could re-evaluate the approach's applicability in different parts of the spectrum. For instance, the approach could already be tested on COSMO-Skymed SAR images acquired in Stripmap acquisition mode in X-band. This archive covers the period from September 2008 to the present with a spatial resolution of 3 m. Finally, the availability of images with an hourly revisit time could allow us to investigate the tidal effects on the positioning of the coastline.

6. REFERENCES

[1] Cappadonia, C., Cafiso, F., Ferraro, R., Martinello, C. and Rotigliano, E., "Rockfall hazards of Mount Pellegrino area (Sicily, Southern Italy)," Journal of Maps **17**(3), 29–39 (2021).

[2] Cappadonia, C., Cafiso, F., Ferraro, R., Martinello, C. and Rotigliano, E., "Analysis of the Rockfall Phenomena Contributing to the Evolution of a Pocket Beach Area Using Traditional and Remotely Acquired Data (Lo Zingaro Nature Reserve, Southern Italy)," Remote Sensing **15**(5), 1401 (2023).

[3] Cafiso, F., Cappadonia, C., Ferraro, R. and Martinello, C., "Rockfall hazard assessment of the Monte Gallo Oriented Nature Reserve area (Southern Italy)," IOP Conf. Ser.: Earth Environ. Sci. **833**(1), 012176 (2021).

[4] Parrino, N., Burrato, P., Sulli, A., Gasparo Morticelli, M., Agate, M., Srivastava, E., Malik, J. N. and Di Maggio, C., "Plio-Quaternary coastal landscape evolution of north-western Sicily (Italy)," Journal of Maps, 1–13 (2023).

[5] Srivastava, E., Malik, J. N., Parrino, N., Burrato, P., Sharma, N., Gadhavi, M., Sulli, A., Di Maggio, C. and Morticelli, M. G., "Extremely fast Holocene coastal landscape evolution in the Kachchh Upland (NW India): Clues from a multidisciplinary review," Journal of Maps, 1–10 (2023).

[6] Parrino, N., Pepe, F., Burrato, P., Dardanelli, G., Corradino, M., Pipitone, C., Morticelli, M. G., Sulli, A. and Di Maggio, C., "Elusive active faults in a low strain rate region (Sicily, Italy): Hints from a multidisciplinary land-to-sea approach," Tectonophysics **839**, 229520 (2022).

[7] Ferranti, L., Burrato, P., Sechi, D., Andreucci, S., Pepe, F. and Pascucci, V., "Late Quaternary coastal uplift of southwestern Sicily, central Mediterranean sea," Quaternary Science Reviews **255**, 106812 (2021).

[8] Sulli, A., Zizzo, E., Spatola, D., Gasparo Morticelli, M., Agate, M., Lo Iacono, C., Gargano, F., Pepe, F. and Ciaccio, G., "Growth and geomorphic evolution of the Ustica volcanic complex at the Africa-Europe plate margin (Tyrrhenian Sea)," Geomorphology **374**, 107526 (2021).

[9] Short, A. D., [Handbook of beach and shoreface morphodynamics], Great Britain: John Wiley; ISBN 0-471-96570-7 (1999).

[10] Patel, K., Jain, R., Patel, A. N. and Kalubarme, M. H., "Shoreline change monitoring for coastal zone management using multi-temporal Landsat data in Mahi River estuary, Gujarat State," Appl Geomat **13**(3), 333–347 (2021).

[11] Bayram, B., Erdem, F., Akpinar, B., Ince, A. K., Bozkurt, S., Catal Reis, H. and Seker, D. Z., "THE EFFICIENCY OF RANDOM FOREST METHOD FOR SHORELINE EXTRACTION FROM LANDSAT-8 AND GOKTURK-2 IMAGERIES," ISPRS Ann. Photogramm. Remote Sens. Spatial Inf. Sci. **IV-4/W4**, 141–145 (2017).

[12] Bengoufa, S., Niculescu, S., Mihoubi, M. K., Belkessa, R. and Abbad, K., "ROCKY SHORELINE EXTRACTION USING A DEEP LEARNING MODEL AND OBJECT-BASED IMAGE ANALYSIS," Int. Arch. Photogramm. Remote Sens. Spatial Inf. Sci. **XLIII-B3-2021**, 23–29 (2021).

[13] Dardanelli, G., Maltese, A., Pipitone, C., Pisciotta, A. and Lo Brutto, M., "NRTK, PPP or Static, That Is the Question. Testing Different Positioning Solutions for GNSS Survey," Remote Sensing **13** (2021).

[14] Lee, J.-S. and Pottier, E., [Polarimetric Radar Imaging: From Basics to Applications], CRC Press (2017).

[15] Maltese, A., Capodici, F., Corbari, C., Ciraolo, G., La Loggia, G. and Sobrino, J. A., "Critical analysis of the thermal inertia approach to map soil water content under sparse vegetation and changeable sky conditions," presented at SPIE Remote Sensing, 23 October 2012, Edinburgh, United Kingdom, 85310T.

[16] Maltese, A., Bates, P. D., Capodici, F., Cannarozzo, M., Ciraolo, G. and La Loggia, G., "Critical analysis of thermal inertia approaches for surface soil water content retrieval," Hydrological Sciences Journal **58**(5), 1144–1161 (2013).